

# Synthesis, characterization, electrochemical and spectroscopic studies of two new heteroleptic Ru(II) polypyridyl complexes

Kasim Ocakoglu<sup>a</sup>, Ceylan Zafer<sup>a</sup>, Bekir Cetinkaya<sup>b</sup>, Siddik Icli<sup>a,\*</sup>

<sup>a</sup> Solar Energy Institute, Ege University, 35100 Bornova, Izmir, Turkey

<sup>b</sup> Department of Chemistry, Faculty of Science, Ege University, 35100 Bornova, Izmir, Turkey

Received 1 June 2006; accepted 12 June 2006

Available online 23 August 2006

## Abstract

New [Ru(L1)(H<sub>2</sub>dc bpy)(NCS)<sub>2</sub>] [K30] and [Ru(L2)(H<sub>2</sub>dc bpy)(NCS)<sub>2</sub>] [K27] complexes were synthesized in a one-pot reaction starting from [RuCl<sub>2</sub>(*p*-cymene)]<sub>2</sub>, where the ligands (H<sub>2</sub>dc bpy = 4,4'-dicarboxy-2,2'-bipyridine, L1 = 4,5-diazafluoren-9-one, and L2 = 1,10-phenanthroline-5,6-dione) are introduced sequentially. The resulting complexes were characterized by UV–vis, emission, IR, TGA, NMR, elemental analysis and cyclic voltammetry. The absorption and emission maxima of the two complexes are very similar to one another. The low-energy MLCT absorption maxima of the complexes appear at 524 nm, and the luminescence consists of a single band with a maximum at 700 and 720 nm, respectively, in DMF solution at 298 K. The electrochemical behaviors of the complexes have been studied in CH<sub>3</sub>CN by cyclic voltammetry. The LUMO energy levels of K27 and K30 were determined as –4.01 and –3.86 eV, respectively. The thermogravimetric analyses (TGA) of the prepared complexes show that the dyes are stable up to about 220 °C. Photodecompositions of the complexes in solution were studied in both ethanol and DMF solvents with a steady-state spectrofluorimeter in time-based mode. The photostability of the compounds in DMF was found to increase twice in comparison to ethanol. Fluorescence quenching experiments of the one simple derivative of PDIs (*N,N'*-bis(1-ethylpropyl)perylene-3,4,9,10-tetracarboxylic acid (EP-PDI)) in DMF were studied vs. increasing K27 and K30 concentrations to monitor donor/acceptor capability. The rate constants (*k<sub>q</sub>*) of EP-PDI for each complex, K27 and K30, were determined as 7.72 × 10<sup>12</sup> and 6.52 × 10<sup>12</sup> M<sup>-1</sup> s<sup>-1</sup>, respectively. In addition, the free energies of exothermic photo-electron transfer (ET) processes between EP-PDI and complexes K27 and K30 were calculated to be –62.3 and –57.9 kcal mol<sup>-1</sup>, respectively.

© 2006 Elsevier Ltd. All rights reserved.

**Keywords:** Ruthenium complexes; Polypyridyl complexes; Photosensitizers; Charge transfer sensitizer

## 1. Introduction

Ruthenium(II) bipyridyl complexes have been extensively studied over the last 30 years as a result of their remarkable chemical stability and photophysical properties [1,2]. These chromophores have found use in a wide variety of applications, from solar energy related research [1–7] to molecular wires [8–10], sensors and switches [11], machines [12] and also as therapeutic agents [13]. Ruthenium polypyridyl sensitizers have been the first choice in view of the extensive

knowledge available. Metal-to-ligand charge transfer (MLCT) transitions dominate their visible light absorption and many of their photophysical and redox behaviors in such complexes. The metal-to-ligand charge transfer absorption can be extended to longer wavelengths by appropriate substituent changes on chromophoric ligands [14]. The major focus of this work has been to investigate thiocyanato complexes, in view of their use as photosensitizers, for example, in photoelectrochemical solar cells. However, polypyridyl L1 and L2 ligands are chosen due to their reactive chemical sites. These special ligands have several distinct properties compared to its analogue 2,2'-bipyridine. First, both of them contain a reactive exocyclic ketone. Second, the rigid structure imposed by the central five-member ring means that the two

\* Corresponding author. Tel.: +90 232 388 6025; fax: +90 232 388 6027.

E-mail address: [siddik.icli@ege.edu.tr](mailto:siddik.icli@ege.edu.tr) (S. Icli).

nitrogen atoms are always held in the same direction. Third, strain will be generated in the central five-member ring (for L1) once it coordinates to ruthenium(II). There have been few reports on the synthesis and characterization of heteroleptic complexes of ruthenium starting from a polymeric complex  $\text{Ru}(\text{CO})_2\text{Cl}_2$  [15–17]. The synthetic methodology of such heteroleptic complexes involves several steps, resulting in very low yields. The present study reports the synthesis and characterization of such new sensitizers using a novel synthetic route and a systematic study of their emission, electrochemical, and photoelectrochemical properties.

## 2. Experimental

UV–vis and fluorescence spectra were recorded in a 1 cm path length quartz cell on a Jasco V-530 UV–vis spectrophotometer and PTI-QM1 spectrofluorometer, respectively. The measured emission and excitation spectra were routinely corrected for the wavelength dependent features. Proton and  $^{13}\text{C}$  NMR spectra were measured on a Bruker 400 MHz spectrometer. The reported chemical shifts are against TMS. Infrared spectra were obtained with a Nicolet Magna 550 FT-IR spectrophotometer with the samples dispersed in compressed KBr pellets. Thermal analyses were carried out by Perkin–Elmer thermogravimetric analyzer Pyris 6TGA. Microanalyses (C, H and N) were carried out with CHNS-932 (LECO) elemental analyzer. Electrochemical data were obtained by cyclic voltammetry using a Metrohm 797 VA Computrace processor. The working electrode was a 25  $\mu\text{m}$  Pt microdisk, the auxiliary electrode was a platinum wire, the reference electrode was a silver wire, and the supporting electrolyte was 0.1 M TBAPF<sub>6</sub> (tetrabutylammonium hexafluorophosphate).

All organic solvents used were of puriss quality from Fluka.  $[\text{RuCl}_2(p\text{-cymene})_2]$  and  $\text{NH}_4\text{SCN}$  were purchased from Fluka. 2,2'-Bipyridine-4,4'-dicarboxylic acid ( $\text{H}_2\text{dcbpy}$ ) and 1,10-phenanthroline were purchased from Aldrich. *N,N'*-Bis(1-ethylpropyl)perylene-3,4,9,10-tetracarboxylic acid (EP-PDI) was purchased from Synton. 4,5-Diazafluoren-9-one [18] and 1,10-phenanthroline-5,6-dione [19,20] were synthesized according to the literatures.

### 2.1. Preparation of 4,5-diazafluoren-9-one (L1)

1,10-Phenanthroline (0.056 mol, 10 g) and KOH (0.103 mol, 5.75 g) were added to 500 mL of water and brought to reflux. Potassium permanganate (0.1773 mol, 28 g) in 200 mL of water was added dropwise to the refluxing mixture. After addition, the solution was refluxed for 0.5 h and filtered to remove  $\text{MnO}_2$ . When the solution was cooled, crude 4,5-diazafluoren-9-one precipitated as yellow needles. Recrystallization was carried out from  $\text{CH}_2\text{Cl}_2/\text{Hexane}$ ; 4.55 g, 45% yield. Anal. Calcd for  $\text{C}_{11}\text{H}_6\text{N}_2\text{O}$ : C, 72.52; H, 3.32; N, 15.38. Found: C, 72.88; H, 3.11; N, 15.21%. FT-IR (KBr,  $\text{cm}^{-1}$ ): 3031, 1717, 1558, 1459, 1400, 1264, 1099.  $^1\text{H}$  NMR ( $\text{CDCl}_3$ )  $\delta$  (ppm): 8.77 (d,  $J = 5.08$  Hz, 2H, NCHCH), 7.95 (d,  $J = 7.4$  Hz, 2H, CHCHC), 7.32 (q,  $J = 5.08$  Hz, 2H, CHCHCH).  $^{13}\text{C}$  NMR  $\delta$  (ppm): 189.6

(CCOC), 163.5 (NCCN), 155.4 (NCHCH), 131.6 (CHCHC), 129.5 (CHCCO), 124.9 (CHCHCH).

### 2.2. Preparation of 1,10-phenanthroline-5,6-dione (L2)

1,10-Phenanthroline-5,6-dione was prepared according to a modification of the procedure by Yamada et al. [19]. A mixture of 1,10-phenanthroline (3.65 g, 20.3 mmol) and KBr (24.85 g, 208.8 mmol) was added to 82 mL of  $\text{H}_2\text{SO}_4$  (98%) previously cooled at nitrogen temperature. The mixture was slowly allowed to warm to room temperature and a thick orange paste was obtained; then 45 mL of concentrated  $\text{HNO}_3$  was added dropwise at room temperature. The resulting red solution was heated at 90 °C for 3 h and then poured into water (1 L). The solution was neutralized with  $\text{Na}_2\text{CO}_3$  and extracted with  $\text{CH}_2\text{Cl}_2$ . The yellow extract was dried on  $\text{MgSO}_4$  and the solvent removed in vacuo. The orange-yellow solid was recrystallized from EtOH; 3.72 g; 87% yield. Anal. Calcd for  $\text{C}_{12}\text{H}_6\text{N}_2\text{O}_2$ : C, 68.57; H, 2.88; N, 13.33. Found: C, 68.22; H, 2.91; N, 13.06%. FT-IR (KBr,  $\text{cm}^{-1}$ ): 3060, 1687, 1561, 1459, 1412, 1290, 1087.  $^1\text{H}$  NMR ( $\text{CDCl}_3$ )  $\delta$  (ppm): 9.08 (q,  $J = 1.6$  Hz, 2H, NCHCH), 8.45 (q,  $J = 1.6$  Hz, 2H, CHCHC), 7.55 (q,  $J = 2.8$  Hz, 2H, CHCHCH).  $^{13}\text{C}$  NMR ( $\text{CDCl}_3$ )  $\delta$  (ppm): 178.7 (CCOCOC), 156.7 (NCHCH), 153.1 (NCCN), 137.4 (CHCHC), 128.3 (CHCHCH), 125.7 (CHCC).

The critical point of this procedure is the treatment of the 1,10-phenanthroline/KBr mixture with sulfuric acid: it has to be performed by adding the heterocyclic diamine/KBr mixture to sulfuric acid pre-cooled at liquid nitrogen temperature.

### 2.3. Preparation of $[\text{Ru}(\text{L1})(\text{H}_2\text{dcbpy})(\text{NCS})_2]$ [K30] and $[\text{Ru}(\text{L2})(\text{H}_2\text{dcbpy})(\text{NCS})_2]$ [K27]

In a typical one-pot synthesis of K27 and K30,  $[\text{RuCl}_2(p\text{-cymene})_2]$  (0.1 g, 0.16 mmol) was dissolved in DMF (50 mL) and corresponding ligand [L1 (0.0585 g, 0.32 mmol) for K30 and L2 (0.0672 g, 0.32 mmol) for K27] was then added. The reaction mixture was heated to 60 °C under argon for 4 h with constant stirring. To this reaction flask  $\text{H}_2\text{dcbpy}$  (0.08 g, 0.32 mmol) was added and refluxed for 4 h. Finally, excess of  $\text{NH}_4\text{SCN}$  (0.988 g, 13 mmol) was added to the reaction mixture and the reflux continued for another 4 h. The reaction mixture was cooled down to room temperature and the solvent was removed by using a rotary evaporator under vacuum. Water was added to the flask and the insoluble solid was collected on a sintered glass crucible by suction filtration. The solid was dried under vacuum. The crude complex was recrystallized from methanol and diethyl ether.

#### 2.3.1. $\text{Ru}^{\text{II}}(4,5\text{-diazafluoren-9-one})(4,4'\text{-dicarboxy-2,2'-bipyridyl})\text{-di}(\text{thiocyanate})$ , $[\text{Ru}^{\text{II}}(\text{L1})(\text{H}_2\text{dcbpy})(\text{NCS})_2]$ , [K30]

183 mg, 89% yield. Anal. Calcd for  $\text{RuC}_{25}\text{H}_{14}\text{N}_6\text{O}_5\text{S}_2$ : C, 46.66; H, 2.19; N, 13.06. Found: C, 46.53; H, 2.09; N, 13.15. FT-IR (KBr,  $\text{cm}^{-1}$ ): 3414, 3109, 2789, 2112, 2061, 1711, 1595, 1401, 1371, 786.  $^1\text{H}$  NMR (DMSO)  $\delta$  (ppm): 9.50 (d,  $J = 6$  Hz, 1H, NCHCH), 9.27 (d,  $J = 5.2$  Hz, 1H, NCHCH), 8.44 (s, 1H, CCHC), 8.25 (s, 1H, CCHC), 8.01

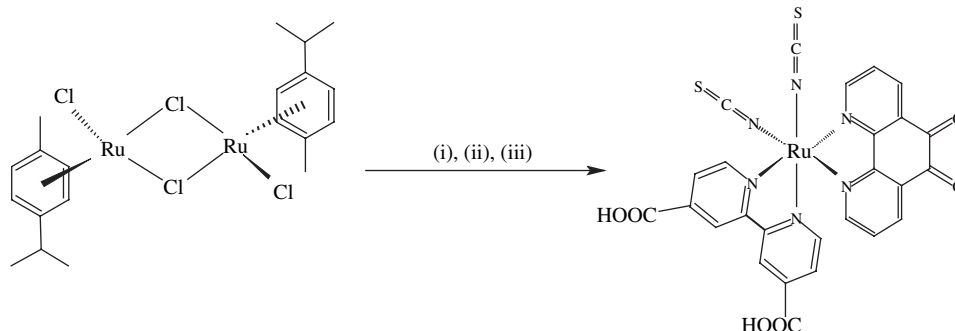
(d,  $J=7.4$  Hz, 1H, CHCHC), 7.84 (d,  $J=7.4$  Hz, 1H, CHCHC), 7.65 (d,  $J=5.2$  Hz, 1H, NCHCH), 7.61 (d,  $J=6$  Hz, 1H, CCHCH), 7.58 (d,  $J=4$  Hz, 1H, NCHCH), 7.13 (q,  $J=5.2$  Hz, 1H, CHCHCH), 7.02 (d,  $J=1.6$  Hz, 1H, CCHCH), 6.49 (q,  $J=5.2$  Hz, 1H, CHCHCH).  $^{13}\text{C}$  NMR (DMSO)  $\delta$  (ppm): 189.8 (CCOC), 172.6 (COOH), 172.3 (COOH), 163.9 (NCCN), 156.5 (NCCN), 155.8 (NCHCH), 155.3 (NCHCH), 143.2 (NCHCH), 142.7 (NCHCH), 140.4 (CHCHC), 140.0 (CHCCH), 139.8 (CHCHC), 139.6 (CHCCH), 135.9 (CCHC), 135.6 (CCHC), 133.2 (NCS), 131.6 (CHCHC), 131.2 (CHCHC), 129.8 (CCOC), 129.6 (CCOC), 125.1 (CHCHCH), 124.6 (CHCHCH).

2.3.2.  $\text{Ru}^{\text{II}}(1,10\text{-phenanthroline-5,6-dione})(4,4'\text{-dicarboxy-2,2'-bipyridyl})\text{-di}(\text{thiocyanate})$ ,  $[\text{Ru}^{\text{II}}(\text{L2})(\text{H}_2\text{dcbpy})(\text{NCS})_2]$ , [K27]

181 mg, 84% yield. Anal. Calcd for  $\text{RuC}_{26}\text{H}_{14}\text{N}_6\text{O}_6\text{S}_2$ : C, 46.50; H, 2.10; N, 12.51. Found: C, 46.22; H, 2.03; N, 12.33. FT-IR (KBr,  $\text{cm}^{-1}$ ): 3402, 3176, 2110, 2065, 1714, 1658, 1633, 1370, 788.  $^1\text{H}$  NMR (DMSO)  $\delta$  (ppm): 9.52 (d,  $J=7.2$  Hz, 1H, NCHCH), 9.48 (d,  $J=1.6$  Hz, 1H, NCHCH), 8.53 (d,  $J=1.6$  Hz, 1H, CCHCH), 8.45 (s, 1H, CCHC), 8.34 (d,  $J=1.6$  Hz, 1H, CCHCH), 8.27 (s, 1H, CCHC), 7.96 (d,  $J=1.6$  Hz, 1H, NCHCH), 7.67 (d,  $J=6.8$  Hz, 1H, CCHCH), 7.61 (d,  $J=4.8$  Hz, 1H, NCHCH), 7.36 (q,  $J=2.8$  Hz, 1H, CHCHCH), 7.05 (d,  $J=1.6$  Hz, 1H, CCHCH), 6.72 (q,  $J=2.8$  Hz, 1H, CHCHCH).  $^{13}\text{C}$  NMR (DMSO)  $\delta$  (ppm): 180.2 (CCOCOC), 179.9 (CCOCOC), 172.7 (COOH), 172.5 (COOH), 157.3 (NCHCH), 156.9 (NCHCH), 156.6 (NCCN), 154.7 (NCCN), 143.4 (NCHCH), 142.9 (NCHCH), 140.6 (CHCHC), 140.1 (CHCCH), 139.8 (CHCHC), 139.4 (CHCCH), 138.6 (CHCHC), 138.1 (CHCHC), 136.1 (CCHC), 135.7 (CCHC), 132.8 (NCS), 129.6 (CHCHCH), 129.2 (CHCHCH), 126.3 (CCOCOC), 126.1 (CCOCOC).

### 3. Results and discussion

A synthetic route starting from the  $[\text{RuCl}_2(p\text{-cymene})]_2$  complex, and using sequential addition of ligands at different time intervals, was designed for the synthesis of heteroleptic polypyridyl ruthenium complexes. Heteroleptic complexes K27 and K30 were prepared as shown in Scheme 1 [21–28].



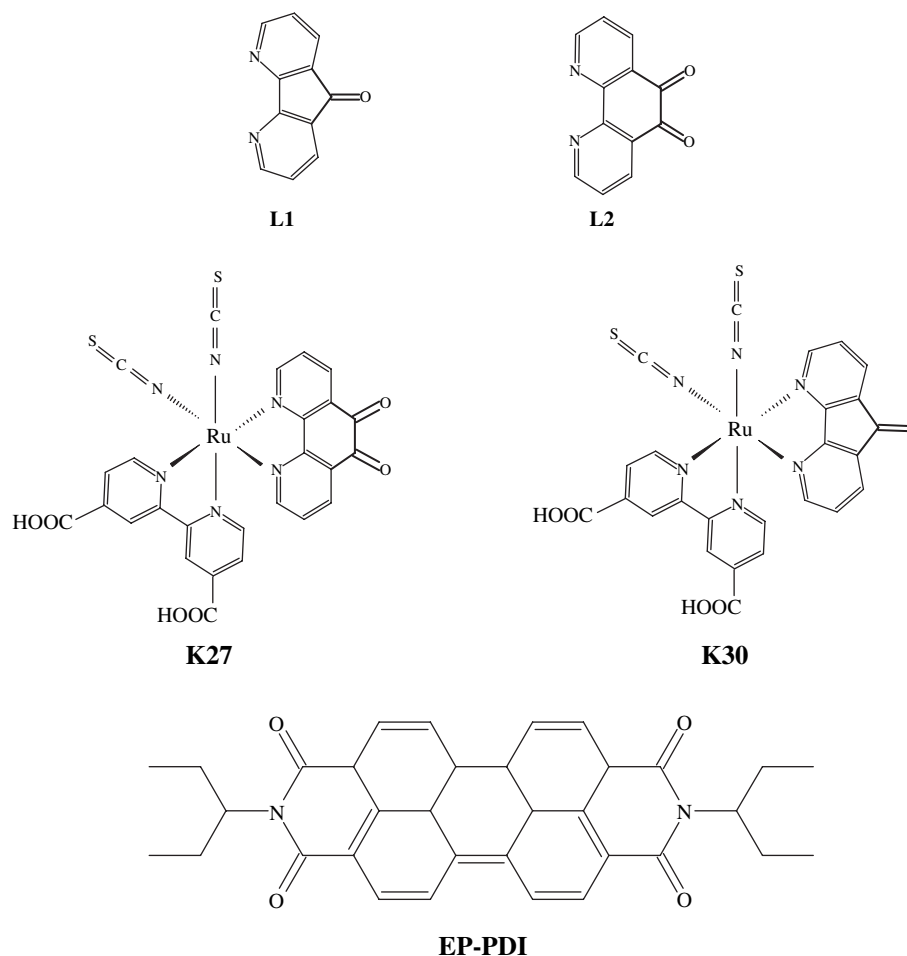
Scheme 1. One-pot synthetic route for K27 dye. (i) DMF, L2, 70 °C, inert atmosphere, and 4 h; (ii) dcbpy, 150 °C, inert atmosphere, and 4 h; (iii)  $\text{NH}_4\text{NCS}$ , 150 °C, inert atmosphere, and 4 h.

This method shown in Scheme 1 is more facile and gives improved yields than previously reported [29]. In the one-pot reaction of the complexes the first step is that the reaction of  $[\text{RuCl}_2(p\text{-cymene})]_2$  dimer with L2 (Scheme 1) in  $N,N'$ -dimethylformamide (DMF) solution at 90 °C results in the mononuclear complex  $[\text{Ru}(\text{L2})\text{Cl}(p\text{-cymene})]\text{Cl}$ . In this step, the coordination of substituted bipyridine ligand to the ruthenium centre takes place with cleavage of the doubly chloride-bridged structure of the dimeric complex. In the second step, mononuclear complex reacts with 4,4'-dicarboxy-2,2'-bipyridine ( $\text{H}_2\text{dcbpy}$ ) in order to give heteroleptic dichloro complex under reduced light at 150 °C. The displacement of the cymene ligand from the coordination sphere of the ruthenium metal by the  $\text{H}_2\text{dcbpy}$  ligand takes place efficiently in organic solvents such as DMF. During the reaction the intermediate products were drawn off and checked by UV–vis spectroscopy. The color change of the solution, from purple to dark red, shows the chloride exchange with  $\text{NCS}^-$  group by the addition of excess of  $\text{NH}_4\text{SCN}$ .

#### 3.1. Absorption and emission studies

The absorption and emission spectra of the complexes are shown in Fig. 1, and the energy maxima and absorption coefficients are summarized in Table 1. The absorption spectra of the resulting complexes K27 and K30 (Scheme 2) were measured in two solvents, DMF and ethanol. The spectrum of complex K27 and K30 in DMF shows two metal-to-ligand charge transfer (MLCT) bands which are well-resolved [30] at 524 and 380 nm, with a molar extinction coefficient of 10 600 and 10 300  $\text{M}^{-1}\text{cm}^{-1}$ , respectively. These results are very close to the reported MLCT absorptivities of other similar complexes [31]. The bands at 304 and 306 nm are assigned to the intraligand  $\pi-\pi^*$  transition of  $\text{H}_2\text{dcbpy}$  and phen/fluoren ligands.

The emission spectra of the complexes were recorded in DMF at room temperature (Fig. 1). Emission of  $\text{Ru}(\text{II})$  polypyridine complexes usually occurs from the lowest-lying  $^3\text{MLCT}$  excited state [1,2,32,14]. When excited at the 400 nm (MLCT absorption band for both complexes), K27 and K30 in DMF solution at 298 K exhibit a luminescence consisting of a single band with a maximum at 700 and



Scheme 2. Structures of the compounds.

720 nm, respectively (Fig. 1a and b). Excitation of these complexes at different wavelengths within the manifold of the MLCT bands gave the same emission maxima. This phenomenon shows that exciting the complex between 350 and 600 nm leads to population of the same luminescent state.

### 3.2. IR spectra

Further structural characterization of K27 and K30 was carried out by IR spectroscopy. The high resolution spectrum exhibits a doublet with peaks at 2110 and 2065  $\text{cm}^{-1}$  for K27, and 2112 and 2066  $\text{cm}^{-1}$  for K30, which is characteristic of the *cis*-configuration of the two thiocyanate ligands. The NCS<sup>-</sup> group has two characteristic modes,  $\nu(\text{N}=\text{C})$  and  $\nu(\text{C}=\text{S})$ , which are frequently considered as diagnostic with respect to the coordination mode of the ambidentate NCS ligand [33]. Furthermore, the N-coordination of the thiocyanate group is confirmed by the presence of the  $\nu(\text{C}=\text{S})$  vibrational band at 780  $\text{cm}^{-1}$ . If the thiocyanate groups were coordinated to ruthenium through their sulfur atoms, a weak  $\nu(\text{C}=\text{S})$  vibrational band around 700  $\text{cm}^{-1}$  would have appeared [34,35]. The fact that such a band was not observed excludes the presence of any significant amount of S-coordinated species in the product. It can be clearly said that the N-coordination of the

thiocyanate group is bound to the metal because of the peaks which are observed at 788 for K27 and 786 for K30. The one broad band at 1714 for K27, and 1711 for K30 are due to the presence of protonated carboxyl groups.

### 3.3. NMR spectroscopy

In Tris-heteroleptic complexes, the symmetry is lowered  $C_1$  when compared to homoleptic complexes ( $D_3$ ). Hence, the NMR spectrum of Tris-heteroleptic complexes is expected to be much more complicated [36]. In complexes K27 and K30, two halves of each ligand are necessarily in different magnetic environments. The NMR spectrum of K27 and K30 in the aromatic region shows 12 resonance peaks. Those 12 well-resolved resonance peaks corresponding to six different aromatic ring protons of H<sub>2</sub>dcby and six different aromatic protons of 1,10-phenanthroline-5,6-dione (for K27) and 4,5-diazafluoren-9-one (for K30). The <sup>13</sup>C NMR spectroscopy proved to be the most valuable tool for determining the geometric configuration of the ruthenium complexes and the linkage properties of the NCS ligand. The proton decoupled <sup>13</sup>C NMR spectra of *cis*- and *trans*-isomers show different carbon resonances that were identified by comparing with known bipyridine complexes [37]. In the aromatic region

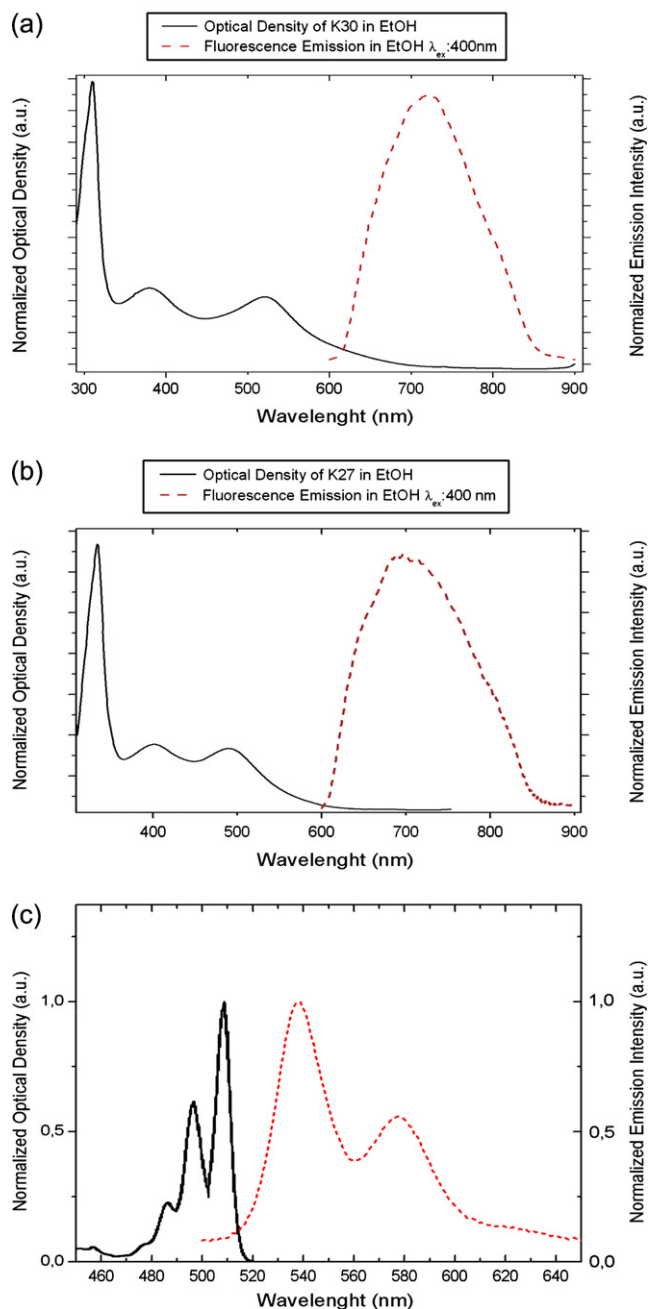


Fig. 1. UV-vis absorption and emission spectra of K30 (a) K27 (b) complexes and EP-PDI (c) measured at 298 K under aerobic conditions in DMF solution.

( $\delta$ , 190–120 ppm), complex K27 shows 23 resonance signals corresponding to 23 carbons of H<sub>2</sub>dc bpy and 1,10-phenanthroline-5,6-dione ligands, whereas complex K30 exhibits only 22 resonance peaks coming from H<sub>2</sub>dc bpy and 4,5-diazafluoren-9-one ligands. It has been reported that S-coordination of the NCS ligand to transition metals shields the carbon atom much more than N-coordination. S-coordinated NCS ligands show carbon resonances at 120–125 ppm [38]. The single resonance peak at 132.8 (for K27) and 133.2 (for K30) was assigned to the carbon of N-coordinated NCS. The two downfield resonances at 172.7–172.5 (for K27) and 172.6–172.3 are assigned to the carboxylate carbons.

Table 1  
UV-vis spectral data for ruthenium complexes

Complex	$\lambda_{\max}$ (nm) ( $\epsilon/10^4 \text{ M}^{-1} \text{ cm}^{-1}$ ) <sup>a</sup>	$\lambda_{\max}$ (nm) ( $\epsilon/10^4 \text{ M}^{-1} \text{ cm}^{-1}$ ) <sup>b</sup>
K27	524 (1.06), 380 (1.11), 304(3.18)	518 (1.02), 376 (1.09), 306 (3.13)
K30	524 (1.03), 380 (1.07), 306 (3.26)	516 (1.02), 378 (1.04), 308 (3.21)

<sup>a</sup> In DMF.

<sup>b</sup> In C<sub>2</sub>H<sub>5</sub>OH,  $T = 298 \pm 1$  K. Errors:  $\lambda_{\max}$ ,  $\pm 1$  nm;  $\epsilon$ ,  $\pm 0.1 \text{ M}^{-1} \text{ cm}^{-1}$ .

### 3.4. Thermal analyses

The thermogravimetric analyses (TGA) of the prepared complexes and ligands were measured under nitrogen atmosphere in the range 20–1000 °C in order to investigate the thermal stability. Fig. 2 shows the TG traces for the ligands (L1, L2) and the new complexes (K30, K27). According to TG traces, the dyes are stable up to about 220 °C and do not undergo any detectable change (Fig. 2). For both complexes, the degradation starts with breaking of the carbonyl groups of the ligands. Fifty percent of mass of compounds K30 and K27 were lost at 650 and 780 °C, respectively. The weight loss of the ligands (L1, L2) were completed up to 320 °C and carbonaceous residue values of them were found to be ~1%. On the other hand, Fig. 2 indicates that the weight loss of the complexes did not complete up to 1000 °C, so they need high temperatures to achieve decomposition. Furthermore, the weight loss of the compounds K30 and K27 were found to be 66 and 63% at 1000 °C, respectively. Furthermore, previous studies about the thermal stabilities of ruthenium (II) complexes carried out in Grätzel group suggest the similar results [39].

### 3.5. Electrochemistry

The electrochemical behaviors of the complexes have been studied in CH<sub>3</sub>CN by cyclic voltammetry. Results are shown in Table 2. All redox potentials were calibrated vs. SCE (Fc = 0.44 V vs. SCE). The cyclic voltammogram of complex K30 shows a quasi-reversible couple at 0.86 V vs. SCE, which can be readily assigned to the Ru(II/III) couple. In complex

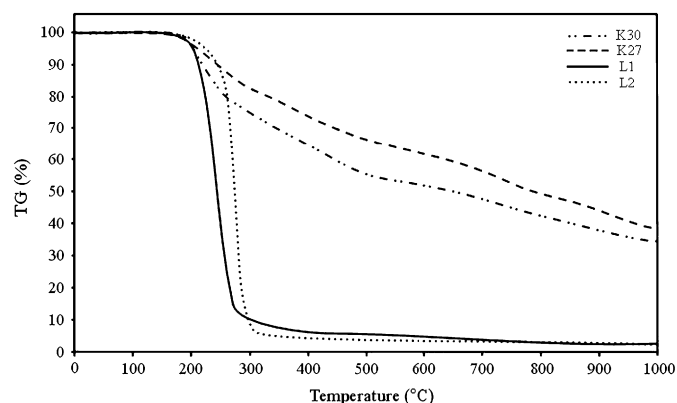


Fig. 2. TG curves of ligands and complexes.

Table 2  
Redox potentials for K27, K30 and EP-PDI<sup>a</sup>

Complex	$E_{\text{red}2}$ (V)	$E_{\text{red}1}$ (V)	$E_{\text{ox}}$ (V)	$E_{\text{Fc}}$ (V)	HOMO (eV)	LUMO (eV)
K27	-1.06	-0.35	0.84	0.44	-5.20	-4.01
K30	-1.03	-0.50	0.86	0.44	-5.22	-3.86
EP-PDI	-0.70	-0.50	1.40	0.44	-6.16	-3.83

<sup>a</sup> All complexes were measured in 0.1 M  $[\text{CH}_3(\text{CH}_2)_3]_4\text{NPF}_6\text{-CH}_3\text{CN}$ , error in potentials  $\pm 0.02$  V;  $T = 23 \pm 1$  °C; scan rate =  $100 \text{ mV s}^{-1}$  ( $E_{\text{red}}$  and  $E_{\text{ox}}$ /V vs. SCE) HOMO (eV) vs. vacuum.

K27, the Ru(II/III) couple was observed at 0.84 V. For an analogous 2,2'-bipyridine ruthenium complex, Meyer et al. reported 0.55 V vs. SCE [40]. The difference (0.31 V) in the oxidation potential of complex K30 from that of the 2, 2'-bipyridine complex is due to the  $\pi$ -accepting nature of  $\text{H}_2\text{dcbpy}$ . There is no considerable difference in the oxidation potential between complexes K27 and K30 due to the  $\pi$ -acceptor strength of the thiocyanate ligands. The low-energy MLCT transitions in these complexes are consistent with Ru(II/III) oxidation potentials.

There are two reversible reductions of complexes K30 and K27. The first reductions were observed at  $-0.35$  V and  $-0.50$  V vs. SCE and the second reductions were observed at  $-1.06$  V and  $-1.03$  V vs. SCE for K27 and K30, respectively. The first reductions correspond to reductions of carbonyl groups of L1 and L2 and the second reductions correspond to reductions of bipyridyl part of L1 and L2 [41]. The difference between the first reductions related to the number of carbonyl group and different electron accepting behavior of two ligands. The first reduction of K27 at  $-0.35$  V was assessed as a two electron process by peak current comparison due to the inclusion of two carbonyl groups on L2 ligand and it was observed at less negative potential than K30 due to higher electron accepting behavior. If a scan is made to more negative potentials, a reduction peak of  $\text{H}_2\text{dcbpy}$  is observed around  $-1.60$  V vs. SCE. [30]. It can be seen from the calculated HOMO–LUMO energy levels of the complexes from the electrochemical measurements in Table 2. The electrochemical measurements of

Table 3  
Rate constants ( $k_p$ ) and half-lives,  $t_{1/2}$  (h) for photodegradation of K27 and K30

Complex	$k_p$ ( $\text{s}^{-1}$ ), $t_{1/2}$ (h) in EtOH	$k_p$ ( $\text{s}^{-1}$ ), $t_{1/2}$ (h) in DMF
K27	$5 \times 10^{-5}$ , 3.85	$1 \times 10^{-5}$ , 19.25
K30	$6 \times 10^{-5}$ , 3.21	$1 \times 10^{-5}$ , 19.25

$t_{1/2}$  values obtained in seconds were converted to unit of hour.

these complexes show that the LUMO of L1 and L2 are higher than the  $\text{H}_2\text{dcbpy}$ . Therefore, in the excited state the electron is transferred to the L1 and L2 ligands.

### 3.6. Photostability studies

Photodecompositions of K27 and K30 in solution were studied in both ethanol and DMF solvents in concentrations of  $3 \times 10^{-5}$  M with a steady-state spectrofluorimeter in time-based mode. Those solvents are chosen to investigate photodecomposition due to the fact that both are commonly used in the fabrication of ruthenium-type dye-sensitized solar cells. The excitation is performed at 400 nm for the complexes K27 and K30 in both solvents. The photodecomposition data were acquired at the emission wavelength of the compounds. The rate constants and half-life constants for photodegradation of K27 and K30 were estimated from a standard first-order decay process. First-order rate constants estimated from the regression  $-\ln(I/I_0)$  vs. time (s), shown in Fig. 3, and the half-lives for photodegradation together with rate constants are given in Table 3. Both the complexes show approximately the same stabilities at the same solvents. On the other hand, the stability of the compounds in DMF has increased twofold when compared to ethanol and this information may be advantageous in selecting solvents for device fabrication.

### 3.7. Fluorescence quenching studies

The simplest of all chemical reactions is electron transfer; this type of process occurred in the photochemical systems,

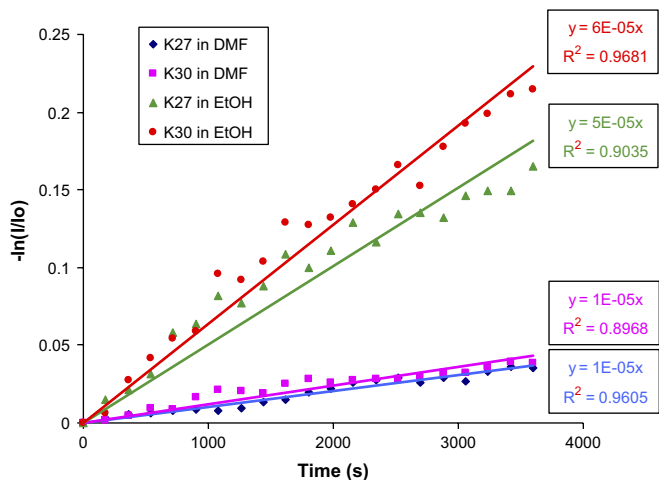


Fig. 3. First-order relations for photodegradation of K27 and K30 in ethanol and DMF solution under Xe-lamp irradiation for 60 min.

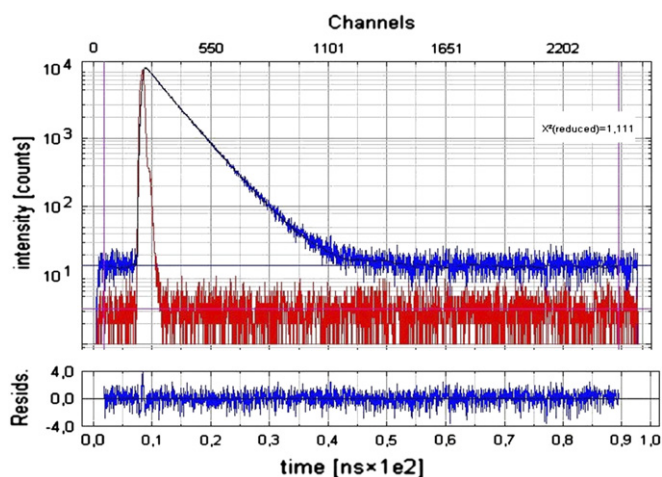


Fig. 4. Fluorescence decay curve of EP-PDI.

where compounds can behave as either donor or acceptor depending upon many factors such as structure of molecule, environment, etc. For example perylenediimides (PDIs) are known to be both electron donors and electron acceptors in literature [42,43]. They behave as electron acceptors toward  $\pi$ -electron rich aromatics such as anthracene, phenanthrene, etc., but behave as an electron donor toward the acceptors such as  $\text{Co}^{2+}$  and KI [43]. Because of this property of PDIs we decided to investigate of photoinduced electron transfer system: perylenediimide/new synthesized ruthenium complexes (PDI/K27 and K30) couple. For this purpose, fluorescence quenching experiments of the one simple commercially available derivative of PDIs (EP-PDI) in DMF were studied vs. increasing K27 and K30 concentrations to monitor donor/acceptor capability. The excitation wavelength was chosen 488 nm, because we observed maximum fluorescence intensity at this wavelength on excitation spectrum. The solutions of  $1 \times 10^{-3}$  M K27 and K30 in DMF were prepared and at each addition 20  $\mu\text{L}$  of these solutions were mixed with  $6.00 \times 10^{-6}$  M 3.0 mL of DMF solutions of EP-PDI dye. The quenching constants,  $k_q$ , were calculated from Stern–Volmer equation (Eq. (1)) [44],

$$\frac{I}{I_0} = 1 + k_q \tau_0 [Q] \quad (1)$$

where  $I_0$  and  $I$  represent the fluorescence intensity of the fluorophore in the absence and presence of quencher with the concentration of  $[Q]$ ,  $\tau_0$  is the radiative lifetime in the absence of

quencher. The slope of the Stern–Volmer plot is equal to  $k_q \tau_0$  and the radiative lifetime  $\tau_0$  of EP-PDI was measured by Time Haarp single photon counting system and defined as 4.25 ns (Fig. 4). The Stern–Volmer plots of EP-PDI for fluorescence quenching with increasing K27 and K30 concentrations are given in Fig. 5. From the slopes of Stern–Volmer plots, the rate constants of EP-PDI for each complex, K27 and K30 were determined to be  $7.72 \times 10^{12}$  and  $6.52 \times 10^{12} \text{ M}^{-1} \text{ s}^{-1}$ , respectively. All  $k_q$  values are higher than the diffusion rate limit reported as  $1 \times 10^{10} \text{ M}^{-1} \text{ s}^{-1}$  by El-Daly [45]. Similar high quenching rates were observed between carbazolocarbazole/triazoles, carbazolocarbazole/perylene diimide couples [46,47]. In all of these systems excited state energy transfer is present. As seen in Fig. 5a and b, EP-PDI fluorescence emission declined by the addition of K27 and K30. Absorption spectra were recorded after each addition of quenchers K27 and K30 to the EP-PDI solution (Fig. 6). These spectra had shown no evidence to the presence of any ground state complexation between EP-PDI and quencher molecules at longer wavelengths. Therefore, the calculations of quenching rate constants ( $k_q$ ) are done using the Stern–Volmer equation (Eq. (1)).

For the solution phase fluorescence quenching experiments, quenching data can be analyzed by using Eq. (2) [48],

$$\Delta G_{\text{ET}} (\text{kcal mol}^{-1}) = 23.06 \left[ E \left( \frac{D^+}{D} \right) \right] - \left[ E \left( \frac{A}{A^-} \right) \right] - E_D^* \quad (2)$$

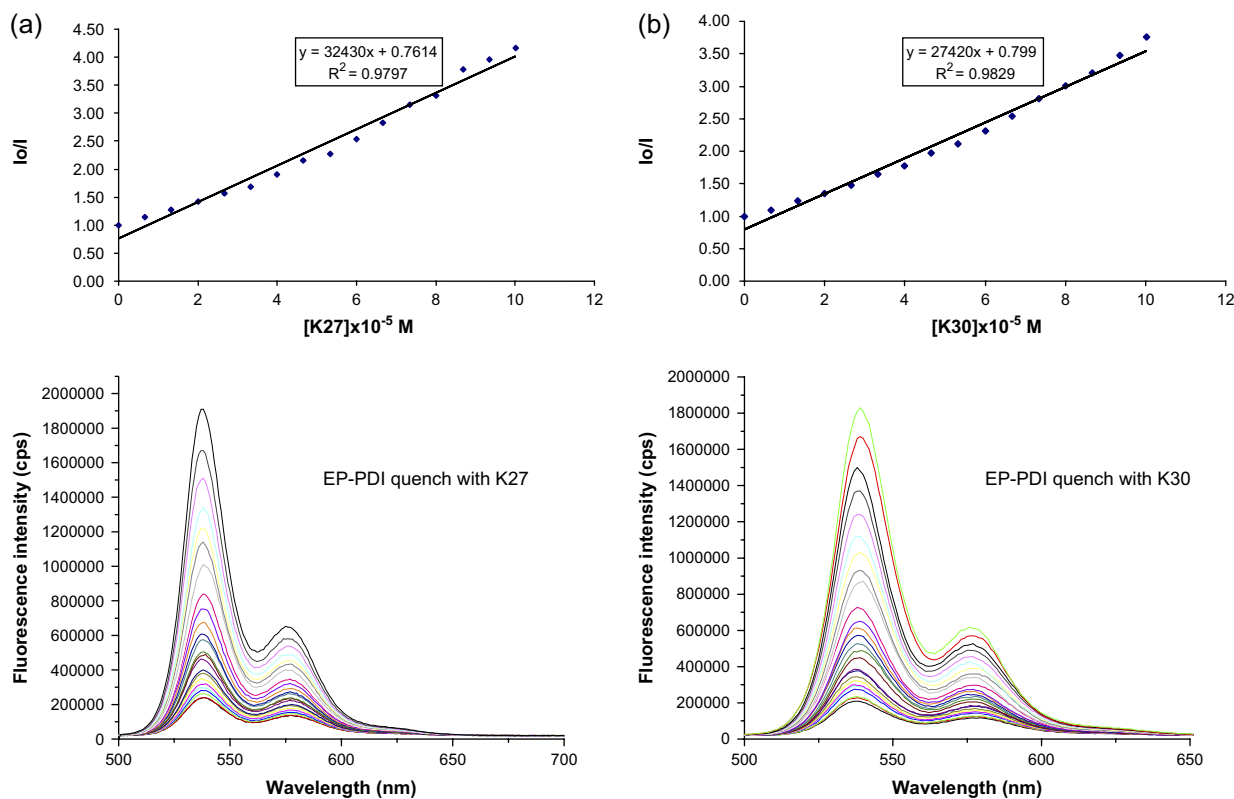


Fig. 5. Stern–Volmer plots of fluorescence emission quenching of (a) EP-PDI with the increase in K27 ( $6.00 \times 10^{-6}$ – $1.00 \times 10^{-4}$  M) concentration and (b) EP-PDI with the increase in K30 ( $6.00 \times 10^{-6}$ – $1.00 \times 10^{-4}$  M) concentration.

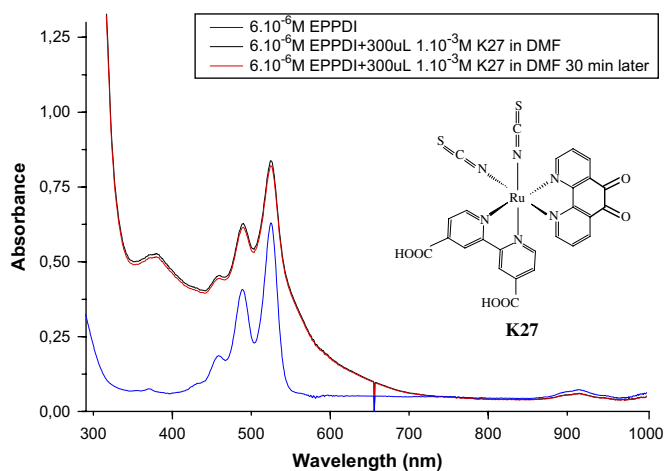


Fig. 6. UV–vis absorption spectra of  $6 \times 10^{-6}$  M EP-PDI solution recorded after 300  $\mu\text{L}$  addition of  $1 \times 10^{-3}$  M K27 solution and 30 min later.

with which the free energy change for an encounter pair undergoing electron transfer is computed by using redox potentials, and where  $E_D^*$  is the excitation energy of the excited state participating in quenching. Redox potentials of K27, K30 and EP-PDI are determined from cyclic voltammetry measurements of the compounds (Figs. 7, 8 and Table 2). The  $\Delta G_{\text{ET}}$  are all below  $-5 \text{ kcal mol}^{-1}$  (the “rule of thumb”, [49]) and may occur for a favorable electron transfer. The free energies of exothermic photo-electron transfer (ET) processes

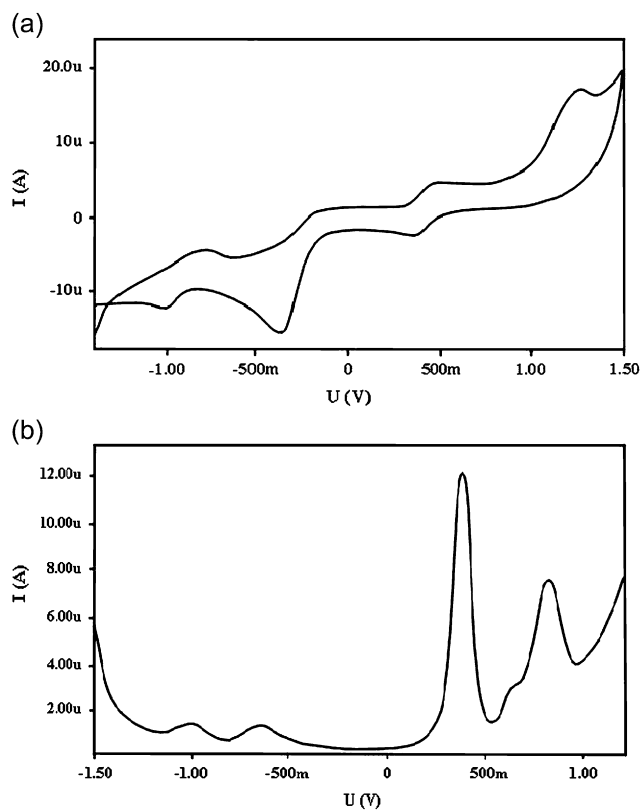


Fig. 7. (a) Cyclic voltammogram of K27. (b) Differential pulse voltammogram of K30.

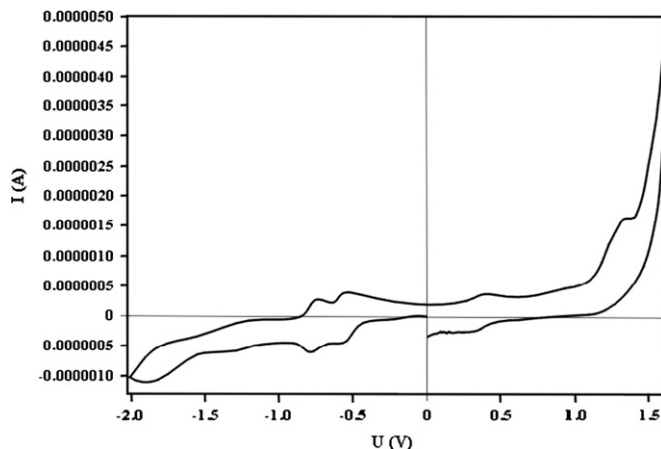


Fig. 8. Cyclic voltammogram of EP-PDI.

between EP-PDI and complexes K27 and K30 were calculated to be  $-62.3 \text{ kcal mol}^{-1}$  and  $-57.9 \text{ kcal mol}^{-1}$  respectively. These results show that there is an electron transfer between EP-PDI and complexes K27 and K30. Relatively lower reduction potentials of K27 and K30 in comparison with EP-PDI were assigned to be favorable for electron transfer. The high electron affinity of carbonyl groups on L1 and L2 makes very easy the electron transfer from ruthenium complex to EP-PDI.

#### 4. Conclusions

Tris–heteroleptic complexes of ruthenium were prepared using a novel synthetic route and characterized with respect to their absorption, luminescence, and redox behavior. The photophysical and redox properties were compared. Fluorescence quenching characteristics of the complexes are directly affected by the high electron affinity of carbonyl groups on L1 and L2. The complexes show characteristic features of strong absorption over a broad spectral range of visible light, which is preferable for efficient solar light energy conversion. Our future plan is to achieve performance studies of these complexes as photosensitizers in the nanocrystalline  $\text{TiO}_2$ -based solar cells. The results of these studies will be published elsewhere.

#### Acknowledgments

We thank The Scientific and Technical Research Council of Turkey (TUBITAK-BAYG), The State Planning Organization of Turkey (DPT), AvH Foundation, Germany for financial supports, and Dr Yusuf Dilgin for his assistance and comments with cyclic voltammetry studies.

#### References

- [1] Juris A, Balzani V, Barigelletti F, Campagna S, Belser P, Zelewsky AV. Ruthenium(II) polypyridine complexes: photophysics, photochemistry, electrochemistry, and chemiluminescence. *Coordination Chemistry Reviews* 1988;277:84–5.

- [2] Kalyanasundaram K. Photochemistry of polypyridine and porphyrin complexes. London: Academic Press Limited; 1992. p. 87–212.
- [3] Campagna S, Pietro CD, Loiseau F, Maubert B, McClenaghan N, Passalacqua R, et al. Recent advances in luminescent polymetallic dendrimers containing the 2,3-bis(2'-pyridyl)pyrazine bridging ligand. *Coordination Chemistry Reviews* 2002;229:67–74.
- [4] Duer H, Bossmann S. Ruthenium polypyridine complexes. On the route to biomimetic assemblies as models for the photosynthetic reaction center. *Accounts of Chemical Research* 2001;34:905–17.
- [5] Meijer MD, Gerard PM, Klink V, Koten GV. Metal-chelating capacities attached to fullerenes. *Coordination Chemistry Reviews* 2002;230:141–63.
- [6] Meyer TJ. Chemical approaches to artificial photosynthesis. *Accounts of Chemical Research* 1989;22:163–70.
- [7] Sun L, Hammarstrom L, Akermarck B, Styring S. Towards artificial photosynthesis: ruthenium–manganese chemistry for energy production. *Chemical Society Reviews* 2001;30:36–49.
- [8] Barigelletti F, Flamigni L. Photoactive molecular wires based on metal complexes. *Chemical Society Reviews* 2000;29:1–12.
- [9] Robertson N, McGowan CA. A comparison of potential molecular wires as components for molecular electronics. *Chemical Society Reviews* 2003;32:96–103.
- [10] Ziessel R, Hissler M, El-Ghayoury A, Harriman A. Multifunctional transition metal complexes. Information transfer at the molecular level. *Coordination Chemistry Reviews* 1998;178(180):1251–98.
- [11] De Silva AP, Gunaratne HQN, Gunnlaugsson T, Huxley AJM, McCoy CP, Rademacher JT, et al. Signaling recognition events with fluorescent sensors and switches. *Chemical Reviews* 1997;97:1515–66.
- [12] Ashton PR, Ballardini R, Balzani V, Credi A, Dress KR, Ishow E, et al. A photochemically driven molecular-level abacus. *Chemistry A European Journal* 2000;6:3558–74.
- [13] Metcalfe C, Thomas JA. Kinetically inert transition metal complexes that reversibly bind to DNA. *Chemical Society Reviews* 2003;32:215–24.
- [14] Meyer TJ. Photochemistry of metal coordination complexes: metal to ligand charge transfer excited states. *Pure and Applied Chemistry* 1986;58:1193–206.
- [15] Black DSC, Deacon GB, Thomas NC. New decarbonylation reactions of carbonylruthenium(II) complexes. *Inorganica Chimica Acta* 1982;65: L75–6.
- [16] Black DSC, Deacon GB, Thomas NC. Ruthenium carbonyl complexes I. Synthesis of  $[\text{Ru}(\text{CO})_2(\text{bidentate})_2]^{2+}$  complexes. *Australian Journal of Chemistry* 1982;35:2445.
- [17] Anderson PA, Strouse GF, Treadway JA, Keene FR, Meyer TJ. Black MLCT absorbers. *Inorganic Chemistry* 1994;33:3863.
- [18] Hendersen LJ, Fronczek FR, Cherry WR. Selective perturbation of ligand field excited states in polypyridine ruthenium(II) complexes. *Journal of the American Chemical Society* 1984;106:5876–9.
- [19] Yamada M, Tanaka Y, Yoshimoto Y, Kuroda S, Shimao I. Synthesis and properties of diamino-substituted dipyrido[3.2-*a*:2',3'-*c*]phenazine. *Bulletin of the Chemical Society of Japan* 1992;65:1006–11.
- [20] Calderazzo F, Marchetti F, Pampaloni G, Passarelli V. Coordination properties of 1,10-phenanthroline-5,6-dione towards group 4 and 5 metals in low and high oxidation states. *Journal of the Chemical Society Dalton Transactions* 1999;4389–96.
- [21] Wang P, Zakeeruddin SM, Moser JE, Nazeeruddin MK, Sekiguchi T, Grätzel M. A stable quasi-solid-state dye-sensitized solar cell with an amphiphilic ruthenium sensitizer and polymer gel electrolyte. *Nature Materials* 2003;2:402–7.
- [22] Freedman DA, Evju JK, Pomije MK. Convenient synthesis of tris-heteroleptic ruthenium(II) polypyridyl complexes. *Inorganic Chemistry* 2001;40:5711–5.
- [23] Strouse GF, Anderson PA, Schnoover JR, Meyer TJ, Keene FR. Synthesis of polypyridyl complexes of ruthenium(II) containing three different bidentate ligands. *Inorganic Chemistry* 1992;31:3004–6.
- [24] Zelewsky AV, Gremaud G. Ruthenium(II) complexes with three different diimine ligands. *Helvetica Chimica Acta* 1988;71:1108–15.
- [25] Juris A, Campagna S, Balzani V, Gremaud G, Zelewsky AV. Absorption spectra, luminescence properties, and electrochemical behavior of tris-heteroleptic ruthenium(II) polypyridine complexes. *Inorganic Chemistry* 1988;27:3652–5.
- [26] Thummel RP, Lefoulon F, Chirayil S. A ruthenium tris(diimine) complex with three different ligands. *Inorganic Chemistry* 1987;26:3072–4.
- [27] Anderson PA, Deacon GB, Harman KH, Keene FR, Meyer TJ, Reitsma DA, et al. Designed synthesis of mononuclear tris(heteroleptic) ruthenium complexes containing bidentate polypyridyl ligands. *Inorganic Chemistry* 1995;34:6145.
- [28] Zakeeruddin SM, Nazeeruddin MK, Humphry-Baker R, Grätzel M. Stepwise assembly of tris-heteroleptic polypyridyl complexes of ruthenium(II). *Inorganic Chemistry* 1998;37:5251–9.
- [29] Zakeeruddin SM, Nazeeruddin MdK, Humphry-Baker R, Péchy P, Quagliotto P, Barolo C, et al. Design, synthesis, and application of amphiphilic ruthenium polypyridyl photosensitizers in solar cells based on nanocrystalline  $\text{TiO}_2$  films. *Langmuir* 2002;18:952–4.
- [30] Nazeeruddin MK, Zakeeruddin SM, Baker RH, Jirousek M, Liska P, Vlachopoulos N, et al. Acid–base equilibria of (2,2'-bipyridyl-4,4'-dicarboxylic acid)ruthenium(II) complexes and the effect of protonation on charge-transfer sensitization of nanocrystalline titania. *Inorganic Chemistry* 1999;38:6298–305.
- [31] Nazeeruddin MK, Kay A, Rodicio I, Humphry-Baker R, Müller E, Liska P, et al. Conversion of light to electricity by *cis*- $\text{X}_2$ bis(2,2'-bipyridyl-4,4'-dicarboxylate)ruthenium(II) charge-transfer sensitizers ( $\text{X} = \text{Cl}^-$ ,  $\text{Br}^-$ ,  $\text{I}^-$ ,  $\text{CN}^-$ , and  $\text{SCN}^-$ ) on nanocrystalline titanium dioxide electrodes. *Journal of the American Chemical Society* 1993;115:6382–90.
- [32] Belser P, Zelewsky AV, Juris A, Barigelletti F, Balzani V. Luminescence of dichlorobis(diimine)ruthenium complexes. *Gazzetta Chimica Italiana* 1983;113:731.
- [33] Wajda S, Rachlewicz K. Spectroscopic properties and bonding character of thiocyanate ligand in some pyridine and 2,2'-dipyridyl ruthenium(II) mixed complexes. *Inorganica Chimica Acta* 1978;31:35–40.
- [34] Nakamoto K. Infrared and Raman spectra of inorganic and coordination compounds. New York: Wiley-Interscience; 1970.
- [35] Herber RH, Nan G, Potenza JA, Schugar HJ, Bino A. Bis(2,2'-bipyridine)bis(isothiocyanato)ruthenium. Solvate (solvate = acetonitrile, DMSO) and related compounds: crystal structure, VTFTIR and NMR study. *Inorganic Chemistry* 1989;28:938–42.
- [36] Orellana G, Alvarez-Ibarra C, Santoro J. Hydrogen-1 and carbon-13 NMR coordination-induced shifts in a series of tris( $\alpha$ -diimine)ruthenium(II) complexes containing pyridine, pyrazine, and thiazole moieties. *Inorganic Chemistry* 1988;27:1025–30.
- [37] Cook MJ, Lewis AP, McAuliffe GSG. Luminescent metal complexes 4-carbon-13 NMR spectra of the tris chelates of substituted 2,2'-bipyridyls and 1,10-phenanthrolines with ruthenium(II) and osmium(II). *Organic Magnetic Resonance* 1984;22:388–94.
- [38] Kohle O, Ruile S, Grätzel M. Ruthenium(II) charge-transfer sensitizers containing 4,4'-dicarboxy-2,2'-bipyridine. Synthesis, properties, and bonding mode of coordinated thio- and selenocyanates. *Inorganic Chemistry* 1996;35:4779–87.
- [39] Amirasr M, Nazeeruddin MdK, Grätzel M. Thermal stability of *cis*-dithiocyanato(2,2'-bipyridyl-4,4'-dicarboxylate)ruthenium(II) photosensitizer in the free form and on nanocrystalline  $\text{TiO}_2$  films. *Thermochimica Acta* 2000;348:105–14.
- [40] Root MJ, Sullivan BP, Meyer TJ, Deutsch E. Thioether, thiolato, and 1,1-dithioato complexes of bis(2,2'-bipyridine)ruthenium(II) and bis(2,2'-bipyridine)osmium(II). *Inorganic Chemistry* 1985;24:2731–9.
- [41] Wang Y, Perez W, Zheng GY, Rillema DP. Syntheses and electrochemical, photophysical, and photochemical properties of ruthenium(II) 4,5-diazafluorenone complexes and their ketal derivatives. *Inorganic Chemistry* 1998;37:2051–9.
- [42] Gregg BA, Sprague J, Peterson MW. Long-range singlet energy transfer in perylene bis(phenethylimide) films. *The Journal of Physical Chemistry B* 1997;101:5362–9.
- [43] Icli S, Demic S, Dindar B, Doroshenko AO, Timur C. Photophysical and photochemical properties of a water-soluble perylenediimide derivative. *Journal of Photochemistry and Photobiology A Chemistry* 2000;136:15–24.

- [44] Turro NJ, Benjamin WA. *Molecular photochemistry*. London; 1965. p. 4–48.
- [45] El-Daly SA. Spectral, lifetime, fluorescence quenching, energy transfer and photodecomposition of *N,N'*-bis(2,6-dimethyl phenyl)-3,4:9,10-perylene-tetracarboxylic diimide (DXP). *Spectrochimica Acta Part A Molecular and Biomolecular Spectroscopy* 1999;55:143.
- [46] İçli S, İcil H, Whitten DG, Sayil Ç, Dityapak İ. Fluorescence quenching between strong  $\pi$ -electron donor–acceptors of carbazolocarbazole and tetrannitrofluorenone leading to electron transfer. *Journal of Luminescence* 1997;75:353–9.
- [47] İçli S, Astley AS, Timur C, Anaç O, Sezer Ö, Dabak K. Fluorescence emission studies on 1-phenyl-4-aryol (and acyl)-1*H*-1,2,3-triazoles. *Journal of Luminescence* 1999;82:41–8.
- [48] Kavarnos GJ, Turro NJ. Photosensitization by reversible electron transfer: theories, experimental evidence, and examples. *Chemical Reviews* 1986;86:401–49.
- [49] Jones G, Griffin SF, Choi CY, Bergmark WR. Electron donor–acceptor quenching and photoinduced electron transfer for coumarin dyes. *The Journal of Organic Chemistry* 1984;49:2705–8.